

Improving Fine-tuning in Composite Higgs Models

Avik Banerjee ^{a,1}, Gautam Bhattacharyya ^{a,2}, Tirtha Sankar Ray ^{b,3}

^{a)} *Saha Institute of Nuclear Physics, HBNI, 1/AF Bidhan Nagar, Kolkata 700064, India*

^{b)} *Department of Physics and Centre for Theoretical Studies, Indian Institute of Technology Kharagpur, Kharagpur 721302, India*

Abstract

In this paper we investigate the next-to-minimal composite Higgs model with a $SO(6)/SO(5)$ coset, whose pNGB sector includes a Standard Model singlet in addition to the usual Higgs doublet. The fermions are embedded in the representation **6** of $SO(6)$. We study the region of parameter space of the model where the radiatively generated potential has global minima with both the doublet and the singlet fields developing vacuum expectation values. We investigate the consequences of kinetic and mass mixing between the Higgs and the singlet scalar that arise in this framework. We demonstrate that the ensuing doublet-singlet mixing can provide a handle to accommodate heavier resonances (top-partners) for a given compositeness scale as compared to the minimal composite Higgs model, thus relaxing the tension with the direct LHC bounds. The main phenomenological consequence of this is a sizable deviation of the Higgs couplings from the Standard Model predictions. While the present experimental precision in the measurement of the Higgs couplings still allows for considerable release of this tension, future measurements of the Higgs branching ratios with increased precision would lead to stringent constraints on this setup.

1 Introduction

The continued absence of new physics at experiments in the energy and intensity frontiers complemented with lack of any pointers from astrophysical experiments have squeezed the space for TeV scale beyond Standard Model physics (BSM) to claustrophobic proportions. However, several theoretical issues like the stability of the weak scale from any high scale dynamics that the Standard Model (SM) might couple to, or the existence of the hyper-charge Landau pole [1] at a trans-Planckian scale demanding nontrivial dynamics at higher scales, indicate that the SM is an effective theory. These and associated theoretical issues remain the main driving force behind the BSM physics. As we enter the precision Higgs era following discovery of the Higgs boson [2, 3] at ~ 125 GeV, in addition to the electroweak precision constraints a set of new constraints from Higgs physics gets imposed on BSM scenarios.

The composite Higgs framework, where the Higgs is identified with a pseudo-Nambu-Goldstone boson (pNGB) originating from spontaneous breaking of a global symmetry in a strongly interacting sector, provides a consistent framework to shield the weak scale from the gauge hierarchy problem [4, 5, 6, 7, 8, 9]. The scale of spontaneous symmetry breaking identified as the compositeness scale separates the weak scale from any higher dynamics. It is the related inexact shift symmetry of the pNGB Higgs that protects the Higgs mass from sensitivity to the UV scale. In these models the Higgs potential

¹avik.banerjeesinp@saha.ac.in

²gautam.bhattacharyya@saha.ac.in

³tirthasankar.ray@gmail.com

is generated at one-loop by the explicit breaking of the global symmetries of the strong sector that is communicated by the linear mixing of the strong sector operators with the SM states. Within this framework of the so called *partial compositeness*, where the potential is generated mainly by top quark induced interactions, the Higgs mass is expected to scale as [10]

$$m_h^2 \sim \frac{N_c}{\pi^2} \frac{m_t^2 m_Q^2}{f^2} \sim \frac{N_c}{\pi^2} y_t^2 \frac{m_Q^2}{\Delta}, \quad (1.1)$$

where m_Q is a generic mass of the strong sector resonances that mix with the top and f is the compositeness scale. The ratio $\Delta \equiv \xi^{-1} \equiv f^2/v_{ew}^2$ is a measure of tuning required to obtain the electroweak vacuum expectation value (vev) of the Higgs (v_{ew}) as compared to the compositeness scale f . In general, the vev-tuning in this class of models is expected to be greater than Δ . In most cases it can be estimated as $\sim \Delta/\kappa$, where $\kappa (\lesssim 1)$ is a model dependent parameter [11, 12, 13, 14, 15]. In this paper we assume that Δ quantifies the *minimal* tuning in the Higgs vev. In fact, we mainly focus on relative tuning between models, where the numerical impact of κ mostly cancels out in ratios. It is clear from Eq. (1.1) that the relative lightness of the Higgs boson requires either a relatively light coloured resonance or a large fine-tuning. The non-observation of any exotic resonance at the LHC [16] implies larger values of Δ and hence more fine-tuned scenario. This is basically a restatement of the more generic observation that the measured Higgs boson mass of ~ 125 GeV is somewhat on the lower side for the otherwise well-motivated composite Higgs framework. This may be contrasted with the supersymmetric extension of the SM where the Higgs mass is perceived to be on the heavier side [17, 18].

The connection of light resonances with composite Higgs mass has been studied extensively in the context of minimal composite Higgs model (MCHM) based on $SO(5)/SO(4)$ coset applying the QCD-like Weinberg sum rules [19, 20, 10, 11, 21], effective two-site models [11] or from explicit calculations with the 5D duals of these theories [22, 23]. Within the MCHM framework the LHC results [16] put severe constraints on the region of parameter space with moderate $\Delta \sim \mathcal{O}(10)$. Interestingly, it was shown that two-loop contributions to the Coleman-Weinberg (C-W) potential from the coloured vector resonances of the strong sector relaxes this by 5 – 10% [24]. Implications of the lepton (τ) resonances on fine-tuning have also been considered [25, 26].

In this paper we explore the possibility of increasing the mass gap between the top-partner resonances and the Higgs boson for a given Δ by employing a possible tree-level doublet-singlet mixing in the pNGB scalar sector of non-minimal model. If the singlet state is heavier, the mixing can lead to a *level-repulsion* pushing the dominantly doublet eigenstate down to match the observed Higgs mass at 125 GeV. The masses of both the states before mixing are conceivably larger and hence more natural from the composite Higgs perspective. The setup is depicted schematically in Fig. 1.1. This possibility naturally demands a larger set of pNGBs in the strong sector than in MCHM, implying an enlargement of the coset space. Many such non-minimal composite Higgs frameworks have been discussed in the literature [27, 28, 29, 30, 31, 32].

Here we will confine ourselves to the next-to-minimal composite Higgs model with a coset $SO(6)/SO(5)$, which would suffice to demonstrate the phenomenon of level-repulsion as a proof of principle. This coset represents the minimal extension beyond MCHM, as it introduces an extra SM gauge-singlet scalar along with the four components of the usual Higgs doublet [27, 33, 34, 35, 36, 37]. Several aspects of this model has been discussed in the literature, e.g. in the context of dark matter [38, 39, 40, 41] and electroweak baryogenesis [42]. Incidentally this also represents the minimal coset that allows for a 4D ultraviolet completion [43, 44, 45, 46, 47, 48]. Here we will be interested in the parameter space

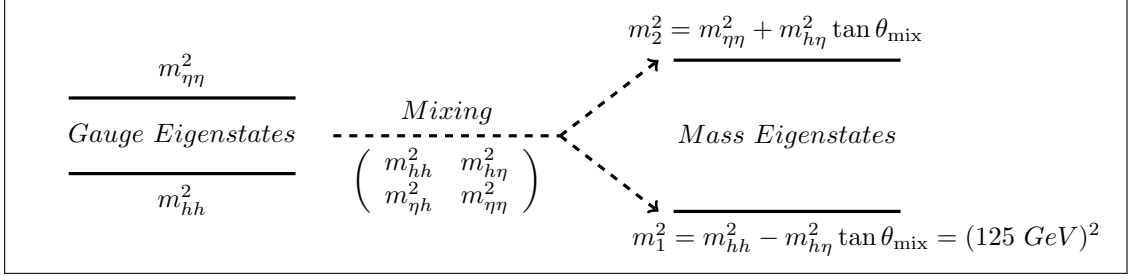


Figure 1.1: *Schematic diagram describing level-repulsion.*

where the radiatively generated C-W potential for the Higgs doublet and the SM singlet minimizes to non-zero vevs for both scalars. This may allow for a nontrivial mixing between the Higgs and the SM singlet in both the kinetic terms and the potential. This is somewhat complementary to most of the studies carried out in the literature for the non-minimal models where the singlet is assumed not to develop a vev making it a possible dark matter candidate. The collider phenomenology of this framework has recently been studied [49].

The paper is organised as follows. In section 2, we briefly review the MCHM, specifically focusing on the rôle of top-partner resonances for reproducing the 125 GeV mass of the Higgs boson. In section 3, we review the next-to-minimal model with $\text{SO}(6)/\text{SO}(5)$ coset and the associated C-W potential. In section 4, we discuss the relaxation in the correlation between the top-partner and the Higgs mass induced by the level-splitting mechanism. Some phenomenological implications are discussed in section 5, before concluding in section 6.

2 Higgs mass and light top-partners in minimal model

In this section we briefly review the C-W scalar potential and the correlation between the light top-partners and the Higgs mass within MCHM. Its coset is $\text{SO}(5)/\text{SO}(4)$ having four pNGBs that can be identified with the components of the SM Higgs doublet. The pNGBs can be parametrised with the non-linear representation (Σ) [50, 51] in the unitary gauge in terms of the dimensionless field h normalised by the compositeness scale (f) as [22]

$$\Sigma = \left(0, 0, 0, h, \sqrt{1-h^2} \right)^T. \quad (2.1)$$

The Higgs potential and the phenomenology of the model depends on the representation into which the SM fermions are embedded. The minimal representation that ensures a custodial protection of the $Zb_L\bar{b}_L$ coupling is the fundamental **5** of $\text{SO}(5)$. Here we confine our discussion to this minimal framework MCHM₅. The most important contribution to the Higgs potential driving electroweak symmetry breaking (EWSB) comes from the top sector. The relevant part of the Lagrangian is given by [10]

$$\mathcal{L} = \bar{t}_L \not{p} \left[\Pi_0^{t_L} + \frac{\tilde{\Pi}_1^{t_L}}{2} h^2 \right] t_L + \bar{t}_R \not{p} \left[\Pi_0^{t_R} + \tilde{\Pi}_1^{t_R} (1-h^2) \right] t_R + \bar{t}_L \left[\frac{M^t}{\sqrt{2}} h \sqrt{1-h^2} \right] t_R + \text{h.c.}, \quad (2.2)$$

where the Π 's are the structure functions which depend on the top-partner masses of the strong sector. The one-loop C-W potential has the structure [7, 52]

$$V_{\text{eff}}(h) = -\frac{\mu^2}{2}h^2 + \frac{\lambda}{4}h^4. \quad (2.3)$$

Minimization of the potential in Eq. (2.3) yields

$$\xi \equiv \langle h \rangle^2 = \frac{\mu^2}{\lambda}. \quad (2.4)$$

The Higgs mass can be expressed in terms of the coefficient λ and the parameter ξ as

$$m_h^2 = \frac{2}{f^2}\xi(1-\xi)\lambda. \quad (2.5)$$

To calculate the parameters of the potential we utilise the Weinberg sum rules to model the structure functions. We employ two strong sector resonances (one singlet and a quadruplet under $\text{SO}(4)$) with masses m_{Q_1} and m_{Q_4} which saturate the integrals. Calculation of the coefficients μ^2 and λ from the top and gauge sectors is described in Appendix A.

In Fig. 2.1 we plot the contours for $m_h = 125$ GeV in the $m_{Q_1} - m_{Q_4}$ plane for $\xi = 0.08$ and 0.04 . The figure suggests that a light Higgs boson implies at least one of the top-partners is relatively light. The present LHC constraints on the top-partners exclude the region below $(m_{Q_1}, m_{Q_4}) \sim 1$ TeV [16]. The situation changes when one embeds the fermions in other representations, see for example [53]. Here we make a passing remark on the issue of double-tuning [21, 11], which eases in cases when there are multiple invariants in the Yukawa structure. In the presence of double-tuning, the total fine-tuning in the Higgs vev can be estimated by Δ/κ , as mentioned previously⁴. In case of MCHM₅, κ can be naïvely parametrised as $\kappa \sim (|F_Q|/m_Q)^2$, where F_Q and m_Q represent the decay constant and mass of the lightest fermionic resonances, respectively. For illustration, a typical estimate shows $\kappa \sim 0.3$ with the resonance mass $m_Q \leq 1.5$ TeV and $\Delta = 10$ [11].

3 Next-to-minimal model: $\text{SO}(6)/\text{SO}(5)$ coset

The next-to-minimal model enlarges the coset to $\text{SO}(6)/\text{SO}(5)$ [27, 46, 54, 34] which includes an additional CP-odd SM singlet along with the usual pNGB Higgs doublet. Interestingly this coset is homomorphic to $\text{SU}(4)/\text{Sp}(4)$. A brief review of the salient features of this model is now in order.

3.1 Parametrization of pNGB degrees of freedom

The spontaneous breaking of global $\text{SO}(6) \rightarrow \text{SO}(5)$, at the composite scale f , delivers five pNGBs. Four of them transform as $(\mathbf{2}, \mathbf{2})$ under $\text{SO}(4) \simeq \text{SU}(2)_L \times \text{SU}(2)_R$, and the other is a singlet of $\text{SO}(4)$ transforming as $(\mathbf{1}, \mathbf{1})$. The pNGBs are parametrised as

$$\Sigma = e^{i\frac{\sqrt{2}}{f}\pi^{\hat{\alpha}}\hat{T}^{\hat{\alpha}}}\Sigma_0 = \frac{1}{\pi}\sin\frac{\pi}{f}\left(\pi_1, \pi_2, \pi_3, \pi_4, \pi_5, \pi\cot\frac{\pi}{f}\right)^T, \quad (3.1)$$

⁴A complementary method based on statistical approach to estimate the fine-tuning can be found in [15].

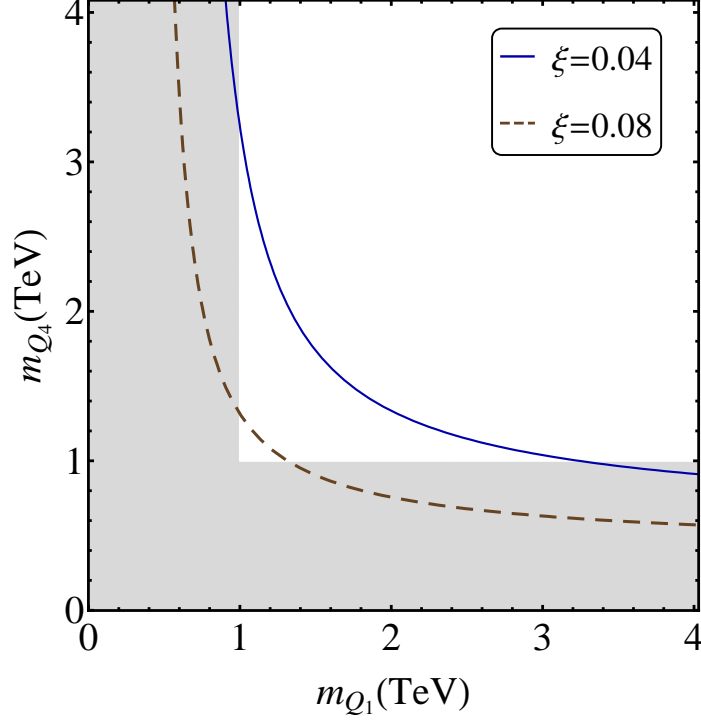


Figure 2.1: The 125 GeV Higgs mass contour in $m_{Q_1} - m_{Q_4}$ plane is displayed for two different choices of ξ . The blue curve corresponds to $\xi = 0.04$ (i.e. $\Delta = 25$), and the brown dashed line corresponds to $\xi = 0.08$ (i.e. $\Delta \simeq 13$). The gray area is already excluded from LHC direct searches.

where $\hat{T}^{\hat{\alpha}}$ are the generators along the broken directions as given in Appendix B, and Σ_0 denotes the vacuum $(0, 0, 0, 0, 1)^T$. In unitary gauge, Σ can be written in terms of a CP-even field, $h \equiv (\pi_4/\pi) \sin(\pi/f)$, and a CP-odd field, $\eta \equiv (\pi_5/\pi) \sin(\pi/f)$, as [38]

$$\Sigma = \left(0, 0, 0, h, \eta, \sqrt{1 - h^2 - \eta^2} \right)^T. \quad (3.2)$$

3.2 Gauge sector and kinetic mixing

The kinetic term for the pNGBs can be written as

$$\mathcal{L}_{\text{kinetic}} = \frac{f^2}{2} (D_\mu \Sigma)^T (D_\mu \Sigma), \quad (3.3)$$

where the covariant derivative is $D_\mu = (\partial_\mu - igT_L^a W_\mu^a - ig'T_R^3 B_\mu)$, with g and g' as the SM gauge couplings. Expanding the covariant derivatives, we get the complete gauge-kinetic term as

$$\mathcal{L}_{\text{kinetic}} = \frac{f^2}{2} \left[(\partial_\mu h)^2 + (\partial_\mu \eta)^2 + \frac{(h\partial_\mu h + \eta\partial_\mu \eta)^2}{1 - h^2 - \eta^2} + \frac{g^2 h^2}{2} \left(|W|^2 + \frac{1}{2 \cos^2 \theta_w} Z^2 \right) \right]. \quad (3.4)$$

In the region of parameter space where both h and η get vevs, a kinetic mixing between h and η is obtained. This becomes explicit once we write down the Lagrangian in terms of the shifted fields (i.e.

$h \rightarrow h + \langle h \rangle$ and $\eta \rightarrow \eta + \langle \eta \rangle$)

$$\mathcal{L}_{\text{kinetic}} \supset \frac{f^2}{2} \left[\left(1 + \frac{\langle h \rangle^2}{1 - \langle h \rangle^2 - \langle \eta \rangle^2} \right) (\partial_\mu h)^2 + \left(1 + \frac{\langle \eta \rangle^2}{1 - \langle h \rangle^2 - \langle \eta \rangle^2} \right) (\partial_\mu \eta)^2 + \left(\frac{2\langle h \rangle \langle \eta \rangle}{1 - \langle h \rangle^2 - \langle \eta \rangle^2} \right) (\partial_\mu h)(\partial_\mu \eta) \right]. \quad (3.5)$$

The kinetic term can be canonically normalised by a non-unitary rotation of h and η , as is routinely employed in Radion-Higgs scenarios [55, 56, 57] or in the case of kinetic mixing in abelian gauge extensions of the SM [58]. The canonically normalised fields denoted by $\{h_n, \eta_n\}$ are related to the gauge eigenstates by the following redefinitions

$$h = ah_n, \quad \eta = bh_n + c\eta_n, \quad (3.6)$$

where the coefficients are given by

$$a = \frac{1}{f} \sqrt{1 - \langle h \rangle^2}, \quad b = -\frac{1}{f} \frac{\langle h \rangle \langle \eta \rangle}{\sqrt{1 - \langle h \rangle^2}}, \quad c = \frac{1}{f} \frac{\sqrt{1 - \langle h \rangle^2 - \langle \eta \rangle^2}}{\sqrt{1 - \langle h \rangle^2}}. \quad (3.7)$$

The transformation described in Eq. (3.6) is not unique⁵, however the phenomenology of the ensuing theory is independent of this choice.

3.3 Fermion embedding

The radiatively generated potential receives contributions from the gauge and Yukawa sectors. Gauge interactions generate a potential only for the doublet state h . Further, the potential for η is protected by a global $U(1)_\eta$ symmetry, which is isomorphic to a $SO(2)$ rotation in the 5-6 direction of Eq. (3.2) [27, 38]. To generate a potential for η , this $U(1)_\eta$ has to be broken explicitly by the SM Yukawa couplings. This implies that some SM fermions embedded in an incomplete multiplet of $SO(6)$ should be charged under $U(1)_\eta$. In the present analysis, we embed the SM fermions in the fundamental **6** representation of $SO(6)$. Under the group decomposition $SO(6) \supset SO(4) \times SO(2) \simeq SU(2)_L \times SU(2)_R \times U(1)_\eta$, one obtains

$$\mathbf{6} = (\mathbf{2}, \mathbf{2})_0 \oplus (\mathbf{1}, \mathbf{1})_2 \oplus (\mathbf{1}, \mathbf{1})_{-2}, \quad (3.8)$$

where the subscripts denote the η -charge. Note that the two singlets under $SO(4) \simeq SU(2)_L \times SU(2)_R$ in Eq. (3.8) are charged under $U(1)_\eta$ and hence are capable of breaking the symmetry protecting η . The left-handed top quark is embedded into $(\mathbf{2}, \mathbf{2})$ protecting the $Zb_L\bar{b}_L$ coupling [59]. On the other hand, right-handed top quark is embedded as a linear combination in both $(\mathbf{1}, \mathbf{1})$. To generate proper SM hypercharges, we assume that the representation **6** of $SO(6)$ is additionally charged under a global

⁵The general non-unitary rotation is of the form,

$$h = ah_n + d\eta_n, \quad \eta = bh_n + c\eta_n.$$

To calculate the coefficients, we need to put the above transformations back in Eq. (3.5) and demand that, coefficients of $(\partial_\mu h_n)^2$ and $(\partial_\mu \eta_n)^2$ would be 1/2 and that of $(\partial_\mu h_n)(\partial_\mu \eta_n)$ would be zero. Definitely, there are three constraint equations and four variables a, b, c, d . Therefore, no unique solution can be found. We take the special choice $d = 0$ for our analysis. We have checked that the final results do not depend on the choice of the shift.

$U(1)_X$ with $X = 2/3$, and $Y = T_R^3 + X$. Finally, we write down the explicit embeddings for the top quark as

$$Q_L = \frac{1}{\sqrt{2}}(-ib_L, -b_L, -it_L, t_L, 0, 0)^T, \quad (3.9)$$

$$T_R = (0, 0, 0, 0, e^{i\delta}c_\theta t_R, s_\theta t_R)^T, \quad (3.10)$$

where $c_\theta(s_\theta)$ denote the cosine (sine) of an angle θ which is a free parameter [33]. Clearly, $\theta = \pi/4$ and $\delta = \pi/2$, restores the $U(1)_\eta$ in the sense that potential for η is no longer generated from the top sector making it an electroweak axion which is severely constrained from charged kaon decay [60].

3.4 Effective potential

With the top quark being embedded in the fundamental representation of $SO(6)$ as described in Eqs. (3.9) and (3.10) and the nonlinear realization of pNGBs given in Eq. (3.2), one can write down the effective Lagrangian for the top-Higgs sector in terms of the group theoretic invariants. We assume $\delta = \pi/2$ in Eq. (3.10), which considerably simplifies the derived potential without losing any key feature required for the present discussion. The effective Lagrangian is given by

$$\begin{aligned} \mathcal{L} = & \bar{t}_L \not{p} \left[\Pi_0^{t_L} + \frac{\tilde{\Pi}_1^{t_L}}{2} h^2 \right] t_L + \bar{t}_R \not{p} \left[\Pi_0^{t_R} + \tilde{\Pi}_1^{t_R} (c_{2\theta} \eta^2 + s_\theta^2 (1 - h^2)) \right] t_R \\ & + \bar{t}_L \left[\frac{M^t}{\sqrt{2}} h \left(ic_\theta \eta + s_\theta \sqrt{1 - h^2 - \eta^2} \right) \right] t_R + \text{h.c.} \end{aligned} \quad (3.11)$$

As anticipated, the couplings to η are through t_R alone as it has a non trivial η -charge. The effective one-loop potential involving the dimensionless fields h and η obtained from the above Lagrangian can be parametrised as

$$V_{\text{eff}}(h, \eta) = -\frac{\mu_1^2}{2} h^2 + \frac{\lambda_1}{4} h^4 - \frac{\mu_2^2}{2} \eta^2 + \frac{\lambda_2}{4} \eta^4 - \frac{\lambda_m}{2} h^2 \eta^2. \quad (3.12)$$

A detailed calculation of the potential from partial compositeness scenario for the coefficients μ_1 , λ_1 , μ_2 , λ_2 and λ_m are given in Appendix C using the Weinberg sum rules framework. The convergence of integrals involved in μ_1 and μ_2 requires introduction of at least three top-partner resonances, whereas for the calculability of the other three coefficients only two resonances would suffice. The coefficients μ_1 and λ_1 contain gauge as well as top contributions, whereas the rest of the parameters contain only the top contributions. This implies that a generic minimization is expected to yield a non-zero vev for η arising from the negative contribution of the top sector to the η quadratic. On the other hand, the vev of the doublet requires a smart cancellation between the top and gauge sectors. The minimum of the above potential corresponds to

$$\xi \equiv \langle h \rangle^2 = \frac{\lambda_2 \mu_1^2 + \lambda_m \mu_2^2}{\lambda_1 \lambda_2 - \lambda_m^2}, \quad \chi \equiv \langle \eta \rangle^2 = \frac{\lambda_1 \mu_2^2 + \lambda_m \mu_1^2}{\lambda_1 \lambda_2 - \lambda_m^2}. \quad (3.13)$$

Recall, $\xi \equiv v_{\text{ew}}^2/f^2$, where $v_{\text{ew}} = 246$ GeV. Note, $\lambda_1, \lambda_2 > 0$ and $\lambda_1 \lambda_2 - \lambda_m^2 > 0$ ensure stability of the potential. The condition for both h and η to develop vevs implies $\mu_1^2, \mu_2^2 > 0$. Also it follows from Eq. (3.2) that

$$\xi + \chi \leq 1. \quad (3.14)$$

In terms of the canonically normalised fields we obtain the following scalar mass matrix

$$M^2(h_n, \eta_n) = \begin{pmatrix} m_{h_n h_n}^2 & m_{h_n \eta_n}^2 \\ m_{\eta_n h_n}^2 & m_{\eta_n \eta_n}^2 \end{pmatrix} ; \quad (3.15)$$

where

$$m_{h_n h_n}^2 = 2\lambda_1 a^2 \xi + 2\lambda_2 b^2 \chi - 4\lambda_m ab \sqrt{\xi \chi} , \quad (3.16)$$

$$m_{\eta_n \eta_n}^2 = 2\lambda_2 c^2 \chi , \quad (3.17)$$

$$m_{h_n \eta_n}^2 = m_{\eta_n h_n}^2 = 2\lambda_2 bc \chi - 2\lambda_m ac \sqrt{\xi \chi} . \quad (3.18)$$

To avoid tachyonic eigenvalues we impose $m_{h_n h_n}^2, m_{\eta_n \eta_n}^2 > 0$ and $\text{Det}[M^2] > 0$. Clearly a non-zero $m_{h_n \eta_n}^2$ gives rise to mass-mixing between the doublet and singlet. The mass eigenvalues can be calculated as [61]

$$m_{\hat{\eta}} = \sqrt{m_{\eta_n \eta_n}^2 + m_{h_n \eta_n}^2 \tan \theta_{\text{mix}}} , \quad (3.19)$$

$$m_{\hat{h}} = \sqrt{m_{h_n h_n}^2 - m_{h_n \eta_n}^2 \tan \theta_{\text{mix}}} , \quad (3.20)$$

where the doublet-singlet mixing angle θ_{mix} is given by

$$\tan 2\theta_{\text{mix}} = \frac{2m_{h_n \eta_n}^2}{m_{\eta_n \eta_n}^2 - m_{h_n h_n}^2} . \quad (3.21)$$

The eigenvectors corresponding to the eigenvalues $m_{\hat{\eta}}$ and $m_{\hat{h}}$ are given by

$$\begin{aligned} \hat{\eta} &= \cos \theta_{\text{mix}} \eta_n + \sin \theta_{\text{mix}} h_n , \\ \hat{h} &= -\sin \theta_{\text{mix}} \eta_n + \cos \theta_{\text{mix}} h_n . \end{aligned} \quad (3.22)$$

4 Level-splitting mechanism in the SO(6)/SO(5) model

In this section we study the improvement in the tension between the light Higgs mass and the top-partner masses for a given $\Delta = f^2/v_{ew}^2$ within the framework of the next-to-minimal model introduced in the previous section. We focus on the region of the parameter space where this tension is released by the *level-splitting* mechanism that is operative when both h and η develop vevs. We would confine ourselves to the region where the vev of the singlet field η is close to its natural value $\chi \lesssim 1$, a choice which does not considerably worsen the vev-tuning. Thus Δ still notionally represents the minimal vev-tuning in this model.

The potential given in Eq. (3.12) can be minimised using the expressions of Eq. (3.13) as discussed in Appendix C. This yields the mass matrix given in Eq. (3.15) which can be expressed in terms of the masses of the two lightest resonances Q_5 and Q_1 . We will treat $\langle h \rangle^2 = \xi$ and $\langle \eta \rangle^2 = \chi$ as free parameters in our analysis. The decay constants of the vector-like fermionic resonances F^{t_L, t_R} , defined in Appendix C, are measures of compositeness of the left- and right-handed top quarks. The compositeness fractions can be expressed as [52]

$$\sin \phi_L \equiv \frac{|F^{t_L}|}{\sqrt{m_{Q_5}^2 + |F^{t_L}|^2}} , \quad \sin \phi_R \equiv \frac{|F^{t_R}|}{\sqrt{m_{Q_1}^2 + |F^{t_R}|^2}} . \quad (4.1)$$

We further parametrise the ratio of the decay constants by

$$|F^{t_L}| \equiv r |F^{t_R}| . \quad (4.2)$$

The compositeness of t_L is constrained to be smaller than t_R from $Zb\bar{b}$ precision measurements [62], i.e. $r < 1$. The expression for the physical top quark mass can be extracted from Eq. (3.11) as

$$\begin{aligned} m_t^2 &= \frac{|M^t(0)|^2}{2} \xi (\chi c_{2\theta} + (1 - \xi) s_\theta^2) \\ &= \frac{|F^{t_L}|^2 |F^{t_R}|^2}{2m_{Q_1}^2 m_{Q_5}^2} \left[m_{Q_1}^2 + m_{Q_5}^2 - 2m_{Q_1} m_{Q_5} \cos \theta_{\text{phase}} \right] \xi (\chi c_{2\theta} + (1 - \xi) s_\theta^2) , \end{aligned} \quad (4.3)$$

where θ_{phase} corresponds to the phase associated with the decay constants, which are in general be complex. Notice from the above expression that for smaller values of θ_{phase} the top quark has to be more composite in order to generate $m_t \simeq 173$ GeV.

The free parameters in the theory now reduce to $\theta, \xi, \chi, r, \theta_{\text{phase}}$ and the top-partner resonance masses m_{Q_1}, m_{Q_5} . To achieve our goal through the level-splitting mechanism we need to ensure the following conditions:

1. $m_{\eta_n \eta_n}^2 > m_{h_n h_n}^2$.
2. $m_{h_n \eta_n}^2 \neq 0$.
3. The predominantly doublet state (\hat{h}) should have a mass ~ 125 GeV.

Naïvely, one would expect that $m_{\eta_n \eta_n}^2 > m_{h_n h_n}^2$ would necessarily imply $\mu_2^2 > \mu_1^2$. Note that μ_2^2 , being the parameter associated with the singlet field η , receives contribution only from loops involving t_R (which is substantially composite as discussed later in the context of Fig. 5.2b), while μ_1^2 receives contributions from both t_L and t_R loops in addition to a contribution from the gauge bosons. As a result, μ_1^2 can even be larger than μ_2^2 when all the contributions are combined. However, the interplay of λ_1, λ_2 and especially λ_m through Eqs. (3.13), (3.16) and (3.17) can yield a substantial region where $m_{\eta_n \eta_n}^2 > m_{h_n h_n}^2$ is satisfied. To demonstrate the choice of parameters we show the variation of the elements of the mass matrix given in Eq. (3.15) as a function of the associated parameters in Fig. 4.1. As can be understood from the plot in Fig. 4.1a, $m_{\eta_n \eta_n}^2 > m_{h_n h_n}^2$ is satisfied when θ (as defined in Eq. (3.10)) is near 0, $\pi/2$ or π . However, the condition that both the doublet and the singlet receive vevs requires θ to be close to $\pi/2$ ⁶. Note that $m_{h_n h_n}^2$ and $m_{h_n \eta_n}^2$ are not quite sensitive to χ unlike $m_{\eta_n \eta_n}^2$. As demonstrated in Figs. 4.1b and 4.1c, $m_{\hat{h}} \sim 125$ GeV requires $\chi \gg \xi$ and θ_{phase} to be near zero. Further the choice for r is constrained by the measurements of the Higgs couplings at the LHC, as well as meeting the condition $\Pi_0^{t_L, t_R} \simeq 1$. The latter constraints prefer the region where $m_{Q_1} < m_{Q_5}$, which is the region explored in this paper. Choosing these parameters admittedly results in additional tuning in the model. A quantitative estimate of this additional tuning asks for a statistical approach which is beyond the mandate of the present paper. In any case, we already obtain a considerable relaxation in the top-partner masses required to reproduce $m_{\hat{h}} = 125$ GeV for a given compositeness scale, as will be discussed below.

⁶While the doublet vev ensures EWSB, the singlet vev generates doublet-singlet mixing required for level-splitting.

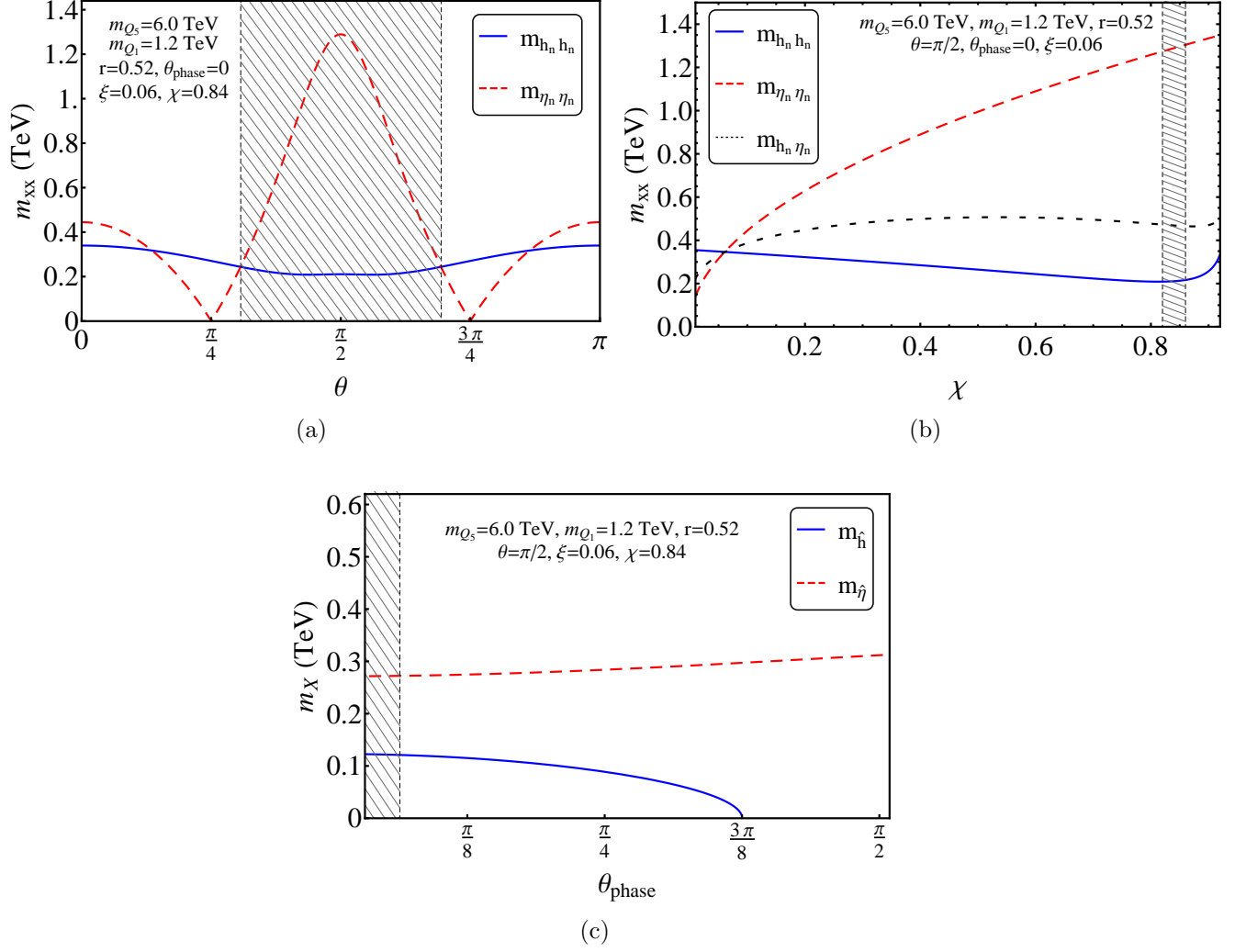


Figure 4.1: Different regions for the model parameters consistent with $m_{\hat{h}} = 125$ GeV are displayed. In panel 4.1a, we show that the condition $m_{\eta_n \eta_n}^2 > m_{h_n h_n}^2$ along with the requirement $\xi \neq 0$, $\chi \neq 0$ are satisfied only in the shaded region around $\theta = \pi/2$. Panel 4.1b shows the variation of the mass matrix elements with the singlet vev χ . The shaded strip corresponds to the range $m_{\hat{h}} = [120-130]$ GeV. In panel 4.1c, the shaded region is consistent with a light Higgs.

In Fig. 4.2a we demonstrate the quantitative impact of level-splitting in the parameter space of the top-partner resonance masses. Guided by the discussion above, we fix the other parameters (see caption of Fig. 4.2a) to zoom into the region where the relaxation of the top-partner masses is most pronounced. The red dashed line is the contour on which the Higgs mass is 125 GeV for the minimal model for $\xi = 0.06$. Here we have mapped $m_{Q_5} \rightarrow m_{Q_4}$ while comparing the contours for the minimal and non-minimal models. For the same ξ , we find that the contour shifts to heavier resonance masses away from the LHC direct search limits. The level-repulsion mechanism is responsible for this shift. The magnitude of this shift depends on the amount of doublet-singlet mixing. Fig. 4.2b shows the Higgs mass contours in the next-to-minimal setup for different choices of ξ .

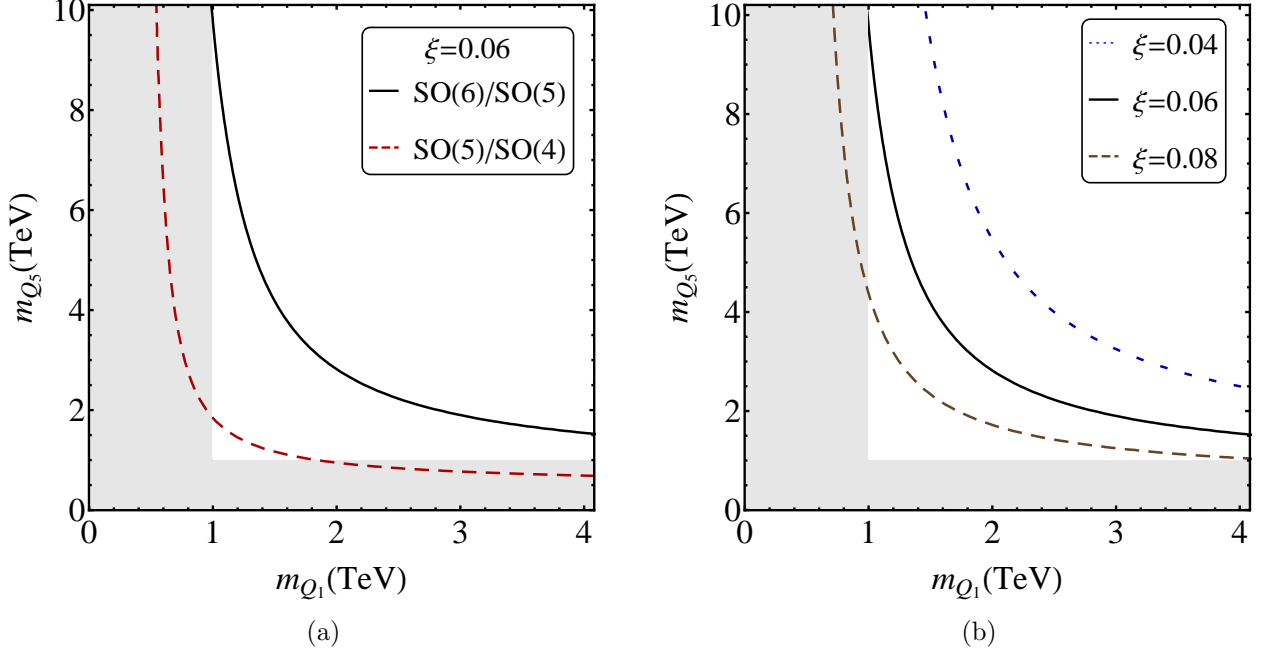


Figure 4.2: In panel 4.2a we show how level-splitting enables relaxation in the parameter space of masses of the top-partners for the same value of ξ . The plot corresponds to $\xi = 0.06$ (i.e. $\Delta \simeq 17$). The red dashed line shows the minimal model $m_{\tilde{h}} = 125$ GeV contour. Gray areas are already excluded by the LHC searches. The black contour refers to the next-to-minimal model. We have fixed $\theta = \pi/2$, $\chi = 0.84$, $r = 0.52$. In panel 4.2b the three different contours are drawn for different values of ξ in the next-to-minimal model, keeping θ , χ and r same as in panel 4.2a. For all cases, the doublet-singlet mixing is kept within $\theta_{\text{mix}} < 0.16$.

The percentage improvement in Δ in this model compared to the minimal model is estimated as

$$\delta_{\text{rel}} = \frac{|\Delta_{\text{SO}(5)/\text{SO}(4)} - \Delta_{\text{SO}(6)/\text{SO}(5)}|}{\Delta_{\text{SO}(5)/\text{SO}(4)}} \times 100\% , \quad (4.4)$$

where for standardization we have kept the masses of the lowest two top-partners identical in both SO(5)/SO(4) and SO(6)/SO(5) setups. In Fig. 4.3a we show the improvement of fine-tuning as a function of the doublet-singlet mixing angle θ_{mix} , defined in Eq. (3.21). In Fig. 4.3b, we plot the mass of the dominantly singlet state with Δ . It is evident from Fig. 4.3b that a smaller Δ can be obtained at the expense of increasing $m_{\tilde{\eta}}$. Also, for the same Δ larger mixing results in smaller $m_{\tilde{\eta}}$, as evident from Eq. (3.21).

5 Phenomenological consequences

In this section we discuss some of the phenomenological consequences of this setup. The doublet-singlet scalar mixing ensures that the Higgs couplings to massive gauge bosons are further suppressed compared to the minimal model. This can provide an avenue to probe and constrain this framework. In the region of parameter space of interest (namely, $m_{\eta_n \eta_n}^2 > m_{h_n h_n}^2$), the top quark (mainly the

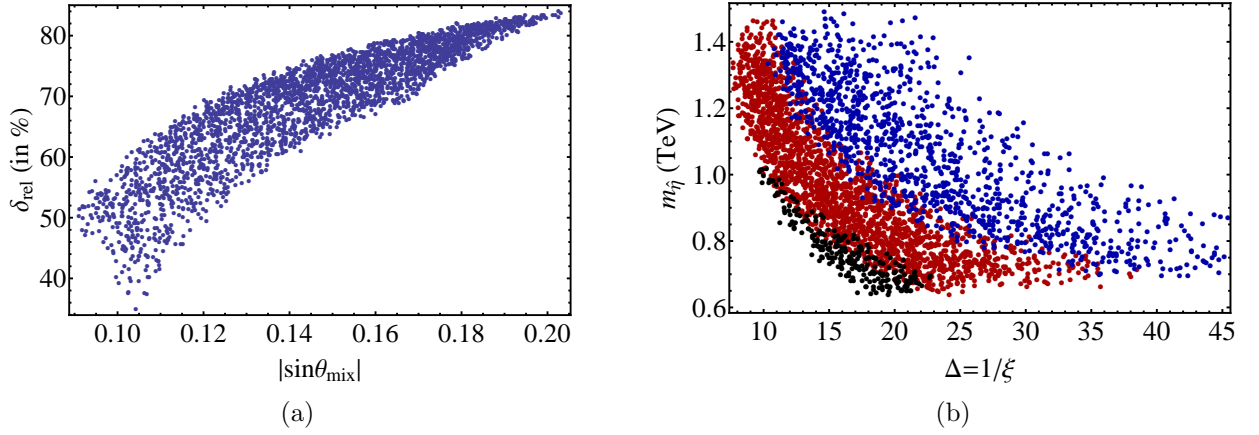


Figure 4.3: The plot on the left panel 4.3a shows the variation of percentage improvement in δ_{rel} , defined in Eq. (4.4), as a function of doublet-singlet mixing. The resonance masses m_{Q_1} and m_{Q_5} are taken in the range between [1.0-1.5] TeV and [5.0-6.0] TeV, respectively and χ is varied within the range [0.4-0.9] keeping $r = 0.52$. In panel 4.3b we have plotted the mass of the heavier singlet-like eigenstate ($m_{\hat{\eta}}$) as a function of Δ . Blue points correspond to $\theta_{\text{mix}} < 0.15$, red to $0.15 < \theta_{\text{mix}} < 0.2$ and black points to $0.2 < \theta_{\text{mix}} < 0.3$. Here, m_{Q_1} and m_{Q_5} are varied in the ranges [1.0-1.2] TeV and [5.5-6.0] TeV, respectively. The parameters χ and r are varied in the ranges [0.75-0.90] and [0.45-0.90], respectively.

right-handed component) turns out to be substantially composite. And finally, the singlet-like state $\hat{\eta}$ is unstable and its decay signatures would leave tangible imprint in colliders.

Constraints on the doublet-singlet mixing come mainly from the Higgs couplings with the gauge bosons. Like in the minimal model, the Higgs couplings to the massive gauge bosons are already suppressed by a factor of $\sqrt{1-\xi}$ with respect to the SM value. On top of that, doublet-singlet mixing induces an additional suppression quantified by θ_{mix} . This suppression can be parametrised as

$$k_V = \frac{g_{\hat{h}VV}}{g_{hVV}^{\text{SM}}} = \cos \theta_{\text{mix}} \sqrt{1-\xi} . \quad (5.1)$$

Within the minimal model, a lower bound $f \gtrsim 700$ GeV [63] was obtained from Higgs physics. This is a somewhat conservative estimate compared to the limit [64] obtained from electroweak precision tests which involve uncertainties stemming from some incalculable UV dynamics. In the next-to-minimal model, the extra suppression strengthens the above limit on f . In fact, we have estimated that with $\theta_{\text{mix}} = 0.2$, the lower bound increases to $f \gtrsim 850$ GeV. For all the parameter choices that have gone into Fig. 4.2, the doublet-singlet mixing is always kept below $\theta_{\text{mix}} = 0.16$, and $f > 850$ GeV (i.e. $\xi < 0.084$). In Fig. 5.1 we present the deviation of the Higgs couplings to massive gauge bosons, defined in Eq. (5.1), with the parameter Δ . The plot shows that even a moderate $\Delta = 10$ is well within the LHC tolerance limit [65]. However, future Higgs branching ratio measurements with higher precision would challenge such tolerance [66, 67]. Additionally, mixing between CP-even and CP-odd states would also have consequences testable in future measurements. It is worth noting that the physical Higgs couplings with the gauge bosons are always suppressed with respect to both the minimal composite model as well as the SM. On the other hand, the coupling of the physical Higgs to the top quark is not necessarily suppressed which may lead to interesting phenomenological consequences.

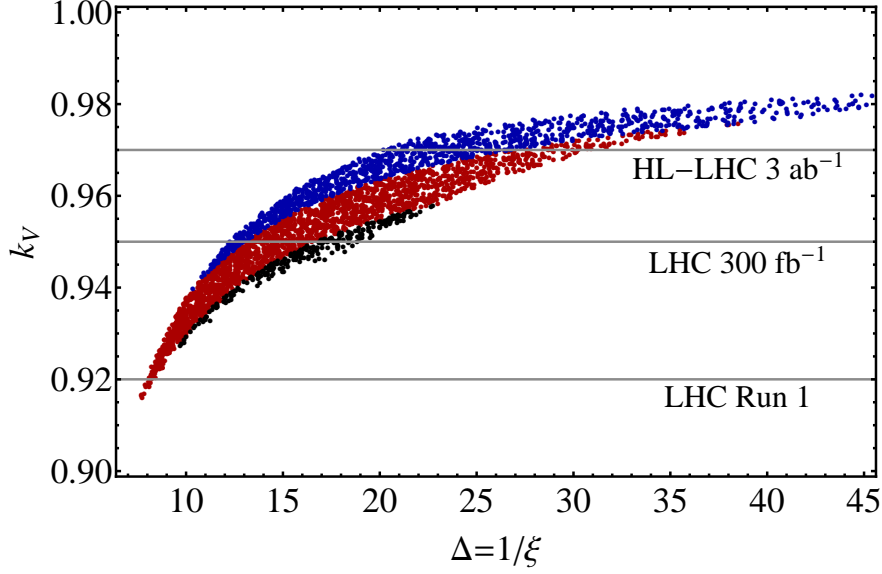


Figure 5.1: The variation of k_V , the modification factor in hVV coupling defined in Eq. (5.1), with the parameter Δ is shown here. The horizontal gray lines represent the 1σ present [65] and anticipated [66, 67] LHC limits with different luminosities. We have varied m_{Q_1} and m_{Q_5} in the ranges [1.0-1.2] TeV and [5.5-6.0] TeV, respectively. The parameters χ and r are varied in the ranges [0.75-0.90] and [0.45-0.90], respectively. For the colours of different scattered points, see caption of Fig. 4.3b (essentially θ_{mix} decreases as we go up).

In Figs. 5.2a and 5.2b, we have plotted the compositeness fraction of t_L and t_R , defined in Eq. (4.1), in the parameter space of the top-partner masses. Note that t_L turns out to be relatively elementary [62]⁷, while t_R is mostly composite in a large region of viable parameter space. Suggested studies to probe the compositeness of t_R [68, 69] would provide another handle to constrain and explore this mechanism.

Finally, we briefly comment on the phenomenology of the additional singlet-like state $\hat{\eta}$, whose detailed collider phenomenology has been studied in [37, 49]. Since it has a small doublet component depending on the mixing parameter θ_{mix} , it has nontrivial coupling to the gauge bosons. It also has a nontrivial coupling to the third generation quarks. If the mass of $\hat{\eta}$ is within the range of the LHC it can be produced in the same way as the 125 GeV Higgs has been produced with the maximum contribution coming from gluon fusion. For large $\hat{\eta}$ mass the production will be suppressed even for sizable mixing. For $m_{\hat{\eta}} > 2m_{\hat{h}}$ and $m_{\hat{\eta}} > 2m_t$, novel channels like $\hat{\eta} \rightarrow \hat{h}\hat{h}$ and $\hat{\eta} \rightarrow t\bar{t}$ would open up. As shown in [49], for the choice of $m_{\hat{\eta}} = 1$ TeV, the production cross section of $\hat{\eta}$ times its branching ratio into $\hat{h}\hat{h}$ channel in LHC (13 TeV) lies in the range (0.01 – 0.1) pb, and the same for $t\bar{t}$ channel is two orders of magnitude smaller. While the CMS and ATLAS exclusion limits on the same quantity for the $\hat{h}\hat{h}$ final states hovers around the predicted upper limit, the experimental exclusion limits for the $t\bar{t}$ channel currently lie substantially above the predicted numbers. As regards the production cross section times the branching ratio in the diphoton channel, the theory prediction for $m_{\hat{\eta}} = 1$ TeV is in the range ($10^{-5} - 10^{-4}$) pb, while the CMS and ATLAS sensitivities lie two orders above.

⁷However, in the region where $m_{Q_1} \sim m_{Q_5}$, t_L appears to be composite. This is a calculational artifact of forcing $r = |F^{t_L}|/|F^{t_R}|$ to fixed values for simplified presentation in the plot and simultaneously determining m_t from Eq. (4.3) using $\theta_{\text{phase}} = 0$. In fact, t_L can be consistently kept mostly elementary by choosing appropriate values of r .

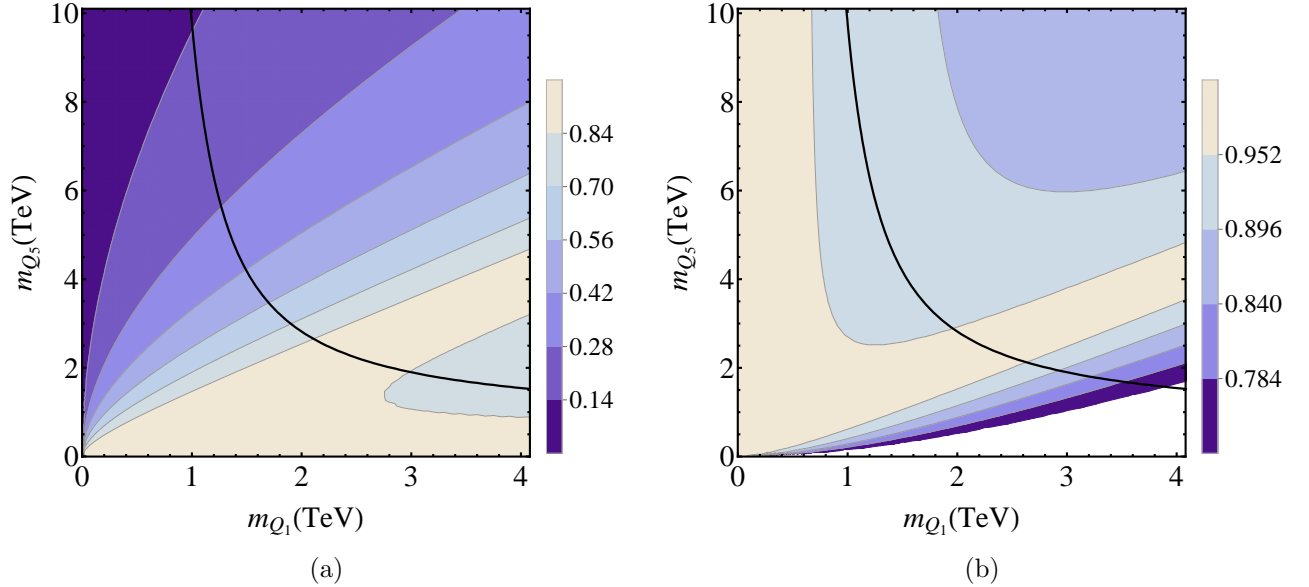


Figure 5.2: The background shades representing the compositeness fractions of t_L and t_R , defined in Eq. (4.1), are shown in Figs. 5.2a and 5.2b, respectively. The value of ξ is fixed at 0.06 for both the plots. The black line refers to $m_h = 125$ GeV, as in Fig. 4.2a.

6 Conclusions

In this paper we have explored the scalar sector of the next-to-minimal composite Higgs model, having a coset $SO(6)/SO(5)$, where the set of pNGB states contains an additional SM singlet compared to the minimal $SO(5)/SO(4)$ model. We demonstrate that a relaxation in the top-partner mass for a given compositeness scale and the measured Higgs mass is achieved in the next-to-minimal model employing the *level-splitting* mechanism. This is operative in a generic minima of the potential where both the doublet and the singlet scalars receive vevs leading to a non-trivial doublet-singlet mixing. Consequently, the relatively lighter doublet-like state becomes even more lighter, to be identified with the observed 125 GeV Higgs boson, while the mass of the singlet-like state is further jacked up. We have performed an extensive scan over the parameter space where the theory is in agreement with all phenomenological constraints. We observe a substantial improvement in the minimal vev-tuning parameter Δ . This improvement can be phrased through the modification of Eq. (1.1), using Eq. (3.20), as follows,

$$m_h^2 \sim \frac{N_c}{\pi^2} y_t^2 \frac{m_Q^2}{\Delta} - m_{h_n \eta_n}^2 \tan \theta_{\text{mix}} , \quad (6.1)$$

where the second term in the right-hand side is necessarily positive. Eq. (6.1) thus allows for a larger value of m_Q compared to what is admissible by Eq. (1.1) for the same choice of Δ . Admittedly, the enhanced naturalness came at the expense of adding an extra singlet scalar which descended from the enlarged coset of the present scenario compared to the minimal model.

There are three main phenomenological consequences of this setup. First, there would be a larger deviation in the Higgs couplings to the W and Z bosons compared to minimal case. The Higgs coupling to the top quark would be modified too. The deviations are still within the LHC limit but would start getting constrained with more precise measurements of the Higgs branching ratios.

Second, the pronounced compositeness of the right-handed top quark that dominates the parameter space of our interest is worth noting. Searches for t_R -compositeness in colliders can be a tool to probe such a mechanism. Finally, the phenomenology of the singlet-like scalar $\hat{\eta}$ would resemble that of the observed Higgs boson *modulo* a significant suppression in its couplings.

Acknowledgments

We thank Tomasz Dutka, Tony Gherghetta and Raymond Volkas for collaboration during the early stages of the project. Discussions with Tony Gherghetta, Aldo Deandrea, Ben Gripaios and Giacomo Cacciapaglia are gratefully acknowledged. We also thank the participants of the Indo-French LIA THEP and CEFIPRA INFRE-HEPNET Kick-off meeting at IISc, Bangalore (2016), for raising concerns on the issue of fine-tuning in composite Higgs models in general. AB acknowledges financial support from Department of Atomic Energy, Government of India. GB acknowledges support of the J.C. Bose National Fellowship from the Department of Science and Technology, Government of India (SERB Grant No. SB/S2/JCB-062/2016). TSR is partially supported by the Department of Science and Technology, Government of India, under the Grant Agreement number IFA13-PH-74 (INSPIRE Faculty Award).

A Effective potential in SO(5)/SO(4) model

The Lagrangian for top-quark (in fundamental representation of SO(5)) is given by

$$\mathcal{L} = \bar{t}_L \not{p} \left[\Pi_0^{t_L} + \frac{\tilde{\Pi}_1^{t_L}}{2} h^2 \right] t_L + \bar{t}_R \not{p} \left[\Pi_0^{t_R} + \tilde{\Pi}_1^{t_R} (1 - h^2) \right] t_R + \bar{t}_L \left[\frac{M^t}{\sqrt{2}} h \sqrt{1 - h^2} \right] t_R + \text{h.c.} \quad (\text{A.1})$$

The top-quark contribution to one-loop C-W potential, obtained using the above Lagrangian can be expressed as

$$V_{\text{top}}(h) = -\frac{\mu_t^2}{2} h^2 + \frac{\lambda_t}{4} h^4. \quad (\text{A.2})$$

The parameters μ_t^2 and λ_t are calculated by integrating over the structure functions. We use the Weinberg sum rules to model the structure functions and introduce minimal set of resonances required to saturate the integrals making them finite. Following two conditions on each of the form factors are needed for the convergence of λ_t :

$$\lim_{q_E^2 \rightarrow 0} q_E^n \frac{\tilde{\Pi}_1^{t_L, t_R}}{\Pi_0^{t_L, t_R}} = 0, \quad (n = 0, 2), \quad (\text{A.3})$$

whereas, to make μ_t^2 calculable, one extra condition is required, which gives rise to one more sum rule:

$$\lim_{q_E^2 \rightarrow 0} \left(\frac{\tilde{\Pi}_1^{t_L}}{2\Pi_0^{t_L}} - \frac{\tilde{\Pi}_1^{t_R}}{\Pi_0^{t_R}} \right) = 0. \quad (\text{A.4})$$

The parameters in the potential can now be calculated as

$$\begin{aligned} \frac{\mu_t^2}{2} = \frac{\lambda_t}{4} &= 2N_c \int \frac{d^4 q_E}{(2\pi)^4} \left[\frac{1}{8} \left(\frac{\tilde{\Pi}_1^{t_L}}{\Pi_0^{t_L}} \right)^2 + \frac{1}{2} \left(\frac{\tilde{\Pi}_1^{t_R}}{\Pi_0^{t_R}} \right)^2 + \frac{|M^t|^2}{2q_E^2 \Pi_0^{t_L} \Pi_0^{t_R}} \right] \\ &= \frac{N_c}{8\pi^2} \frac{m_t^2 m_{Q_1}^2 m_{Q_4}^2}{m_{Q_1}^2 - m_{Q_4}^2} \log \left(\frac{m_{Q_1}^2}{m_{Q_4}^2} \right) \frac{1}{\xi(1-\xi)}, \end{aligned} \quad (\text{A.5})$$

where m_t is the top quark mass and m_{Q_1} and m_{Q_4} represent the masses corresponding to the two lightest top-partners transforming as singlet and quadruplet under $\text{SO}(4)$, respectively. It follows from Eq. (A.5) that, the top-quark contribution alone gives $\xi = 0.5$. The gauge sector contribution on the other hand, enabling a cancellation with fermion contribution, can effectively reduce ξ . Considering both gauge and top contributions, the total potential can be written as

$$V_{\text{eff}}(h) = -\frac{\mu^2}{2} h^2 + \frac{\lambda}{4} h^4 = -\frac{1}{2} (\mu_t^2 - \mu_g^2) h^2 + \frac{1}{4} (\lambda_t - \lambda_g) h^4, \quad (\text{A.6})$$

where [10]

$$\frac{\mu_g^2}{2} = \frac{9}{2} \int \frac{d^4 q_E}{(2\pi)^4} \frac{\Pi_1(-q_E^2)}{4\Pi_0(-q_E^2)} = \frac{9g^2 f^2 m_\rho^2 m_a^2}{128\pi^2 (m_a^2 - m_\rho^2)} \log \left(\frac{m_a^2}{m_\rho^2} \right), \quad (\text{A.7})$$

$$\begin{aligned} \frac{\lambda_g}{4} &= -\frac{9}{2} \int \frac{d^4 q_E}{(2\pi)^4} \frac{\Pi_1(-q_E^2)^2}{32\Pi_0(-q_E^2)^2} = -\frac{9g^4 f^4}{1024\pi^2} \left[\log \left(\frac{m_a m_\rho}{M_W^2} \right) - \frac{(m_a^4 + m_\rho^4)}{(m_a^2 - m_\rho^2)^2} \right. \\ &\quad \left. - \frac{(m_a^2 + m_\rho^2)(m_a^4 - 4m_a^2 m_\rho^2 + m_\rho^4)}{2(m_a^2 - m_\rho^2)^3} \log \left(\frac{m_a^2}{m_\rho^2} \right) \right], \end{aligned} \quad (\text{A.8})$$

where m_a, m_ρ are masses of the vector resonances in the strong sector. These are also expected to be light to account for the perturbative unitarity of the theory [70]. It is crucial to note that, μ_g^2 is always positive. Clearly, to drive EWSB, $\mu_g^2 < \mu_t^2$ is a requirement. The numerical impact of λ_g is small.

B $\text{SO}(6)$ Algebra

We have used the following convention for the generators of $\text{SO}(6)$:

$$\begin{aligned} T^A &= \{T^\alpha, \hat{T}^{\hat{\alpha}}\} = \{T_L^a, T_R^a, T^{\hat{a}}, \hat{T}^{\hat{\alpha}}\}; \\ (A &= 1, \dots, 15; \alpha = 1, \dots, 10; \hat{\alpha} = 1, \dots, 5; a = 1, 2, 3; \hat{a} = 1, 2, 3, 4), \end{aligned}$$

where $\alpha = \{a, \hat{a}\}$ denotes the unbroken indices and $\hat{\alpha}$ denotes the broken indices for $\text{SO}(6) \rightarrow \text{SO}(5)$. The explicit expressions of the generators in fundamental representation of $\text{SO}(6)$ are as follows:

$$(T_{L,R}^a)_{ij} = -\frac{i}{2} \left[\frac{1}{2} \epsilon^{abc} (\delta_i^b \delta_j^c - \delta_j^b \delta_i^c) \pm (\delta_i^a \delta_j^4 - \delta_j^a \delta_i^4) \right], \quad (\text{B.1})$$

$$(T^{\hat{a}})_{ij} = -\frac{i}{\sqrt{2}} (\delta_i^{\hat{a}} \delta_j^5 - \delta_j^{\hat{a}} \delta_i^5), \quad (\text{B.2})$$

$$(\hat{T}^{\hat{\alpha}})_{ij} = -\frac{i}{\sqrt{2}} (\delta_i^{\hat{\alpha}} \delta_j^6 - \delta_j^{\hat{\alpha}} \delta_i^6), \quad (\text{B.3})$$

where i, j run from 1 to 6.

C Effective potential from the top sector for SO(6)/SO(5) model

With the elementary top quark embeddings given in Eqs. (3.9) and (3.10), the effective Lagrangian involving the top quark can be constructed by taking group theoretic invariants as follows,

$$\mathcal{L} = \Pi_0^{tL}(p)\bar{t}_L\not{p}t_L + \tilde{\Pi}_1^{tL}(p)(\bar{Q}_L\Sigma)\not{p}(\Sigma^T Q_L) + \Pi_0^{tR}(p)\bar{t}_R\not{p}t_R + \tilde{\Pi}_1^{tR}(p)(\bar{T}_R\Sigma)\not{p}(\Sigma^T T_R) \\ + M^t(p)(\bar{Q}_L\Sigma)(\Sigma^T T_R) + \text{h.c.} , \quad (\text{C.1})$$

where Σ is given in Eq. (3.2), and the momentum dependent form factors encode the details of the dynamics of composite resonances. Substituting explicit forms of Q_L , T_R and Σ , as given in Eqs. (3.9), (3.10) and (3.2) respectively, the effective Lagrangian takes the following form:

$$\mathcal{L} = \bar{t}_L\not{p}\left[\Pi_0^{tL} + \frac{\tilde{\Pi}_1^{tL}}{2}h^2\right]t_L + \bar{t}_R\not{p}\left[\Pi_0^{tR} + \tilde{\Pi}_1^{tR}(c_{2\theta}\eta^2 + s_\theta^2(1-h^2))\right]t_R \\ + \bar{t}_L\left[\frac{M^t}{\sqrt{2}}h\left(ic_\theta\eta + s_\theta\sqrt{1-h^2-\eta^2}\right)\right]t_R + \text{h.c.} \quad (\text{C.2})$$

This leads to the following one-loop effective Coleman-Weinberg potential:

$$V_{\text{eff}}(h, \eta) = -2N_c \int \frac{d^4 q_E}{(2\pi)^4} \left[\log\left(1 + \frac{\tilde{\Pi}_1^{tL}}{2\Pi_0^{tL}}h^2\right) + \log\left(1 + \frac{\tilde{\Pi}_1^{tR}}{\Pi_0^{tR}}(c_{2\theta}\eta^2 + s_\theta^2(1-h^2))\right) \right. \\ \left. + \log\left(1 + \frac{|M^t|^2}{2q_E^2\Pi_0^{tL}\Pi_0^{tR}}h^2(c_{2\theta}\eta^2 + s_\theta^2(1-h^2))\right) \right] , \quad (\text{C.3})$$

where N_c is the number of QCD colours of the fermions ($N_c = 3$), and q_E denotes the Euclidean momenta. The form factors Π_0 , $\tilde{\Pi}_1$, M^t can be split keeping in mind SO(5) representations as follows,

$$\Pi_0^{tL,tR} = 1 + \Pi_{Q_5}^{tL,tR} , \quad \tilde{\Pi}_1^{tL,tR} = \Pi_{Q_1}^{tL,tR} - \Pi_{Q_5}^{tL,tR} , \quad M^t = M_{Q_1}^t - M_{Q_5}^t . \quad (\text{C.4})$$

Q_1 and Q_5 represent resonances transforming as singlet and five-plet under SO(5), respectively. Now, in view of the results obtained from large-N formalism, form factors encoding strong dynamics can be written as a sum of contributions from infinite number of resonance particles with increasing mass as

$$\Pi_{Q_5}^{tL,tR} = \sum_n \frac{|F_{Q_5^{(n)}}^{tL,tR}|^2}{q_E^2 + m_{Q_5^{(n)}}^2} , \quad \Pi_{Q_1}^{tL,tR} = \sum_n \frac{|F_{Q_1^{(n)}}^{tL,tR}|^2}{q_E^2 + m_{Q_1^{(n)}}^2} , \quad (\text{C.5})$$

$$M_{Q_5}^t = \sum_n \frac{F_{Q_5^{(n)}}^{tL} F_{Q_5^{(n)}}^{*tR} m_{Q_5^{(n)}}}{q_E^2 + m_{Q_5^{(n)}}^2} , \quad M_{Q_1}^t = \sum_n \frac{F_{Q_1^{(n)}}^{tL} F_{Q_1^{(n)}}^{*tR} m_{Q_1^{(n)}}}{q_E^2 + m_{Q_1^{(n)}}^2} . \quad (\text{C.6})$$

The quantities $F^{tL,tR}$ are the decay constants of the corresponding resonances. After expanding all the logarithms the potential can be written as follows,

$$V_{\text{eff}}(h, \eta) = -\frac{\mu_1^2}{2}h^2 + \frac{\lambda_1}{4}h^4 - \frac{\mu_2^2}{2}\eta^2 + \frac{\lambda_2}{4}\eta^4 - \frac{\lambda_m}{2}h^2\eta^2 , \quad (\text{C.7})$$

where the parameters $\mu_1, \lambda_1, \mu_2, \lambda_2$ and λ_m are listed below:

$$\mu_1^2 = 2\alpha_L - 4s_\theta^2\alpha_R + 4s_\theta^4\beta_R + 2s_\theta^2\epsilon, \quad (\text{C.8})$$

$$\lambda_1 = \beta_L + 4s_\theta^4\beta_R + 4s_\theta^2\epsilon, \quad (\text{C.9})$$

$$\mu_2^2 = 4c_{2\theta}\alpha_R - 4s_\theta^2c_{2\theta}\beta_R, \quad (\text{C.10})$$

$$\lambda_2 = 4c_{2\theta}^2\beta_R, \quad (\text{C.11})$$

$$\lambda_m = 4s_\theta^2c_{2\theta}\beta_R + 2c_{2\theta}\epsilon. \quad (\text{C.12})$$

In the above expressions, $\alpha_{L,R}$, $\beta_{L,R}$ and ϵ denote the integrals over the momentum dependent form factors as follows:

$$\alpha_{L,R} = N_c \int \frac{d^4 q_E}{(2\pi)^4} \frac{\tilde{\Pi}_1^{t_L, t_R}}{\Pi_0^{t_L, t_R}}, \quad (\text{C.13})$$

$$\beta_{L,R} = N_c \int \frac{d^4 q_E}{(2\pi)^4} \left(\frac{\tilde{\Pi}_1^{t_L, t_R}}{\Pi_0^{t_L, t_R}} \right)^2, \quad (\text{C.14})$$

$$\epsilon = N_c \int \frac{d^4 q_E}{(2\pi)^4} \frac{|M^t|^2}{q_E^2 \Pi_0^{t_L} \Pi_0^{t_R}}. \quad (\text{C.15})$$

It can be readily observed that, $\beta_{L,R}$ and ϵ become finite if $\tilde{\Pi}_1^{t_L, t_R} \sim \mathcal{O}(1/q_E^4)$, which can be achieved with two resonances only, whereas $\alpha_{L,R}$ become finite if $\tilde{\Pi}_1^{t_L, t_R}$ fall with q_E faster than $\mathcal{O}(1/q_E^4)$. To achieve the latter, minimum three resonances are required. Note that, $\alpha_{L,R}$ are present only in the expressions for μ_1 and μ_2 . Since the scalar mass matrix involves neither of the above mentioned two coefficients, employing only two resonances we can calculate the two scalar masses. The masses of these two resonances (one singlet and another a five-plet of $\text{SO}(5)$) have been denoted by m_{Q_1} and m_{Q_5} . Assuming $\Pi_0^{t_L, t_R} \simeq 1$, the Weinberg sum rules arising from the condition, $\lim_{q_E^2 \rightarrow \infty} q_E^n \tilde{\Pi}_1^{t_L, t_R} = 0$, with $(n = 0, 2)$ lead to

$$|F_1^{t_L, t_R}| = |F_5^{t_L, t_R}| \equiv |F^{t_L, t_R}|. \quad (\text{C.16})$$

Imposing the above condition, the form factors turn out to be

$$\tilde{\Pi}_1^{t_L, t_R} = \frac{|F^{t_L, t_R}|^2 (m_{Q_5}^2 - m_{Q_1}^2)}{(q_E^2 + m_{Q_1}^2)(q_E^2 + m_{Q_5}^2)}. \quad (\text{C.17})$$

To calculate M^t , we make another assumption that $F_1^{t_L, t_R}$ are real, and

$$F_5^{t_L} F_5^{t_R*} \simeq |F^{t_L}| |F^{t_R}| e^{i\theta_{\text{phase}}}. \quad (\text{C.18})$$

With the above assumption

$$M^t = \frac{|F^{t_L}| |F^{t_R}|}{(q_E^2 + m_{Q_1}^2)(q_E^2 + m_{Q_5}^2)} \left[(m_{Q_1} - m_{Q_5} e^{i\theta_{\text{phase}}}) q_E^2 + m_{Q_1} m_{Q_5} (m_{Q_5} - m_{Q_1} e^{i\theta_{\text{phase}}}) \right]. \quad (\text{C.19})$$

Employing all these relations, the integrals $\beta_{L,R}$ and ϵ can be evaluated exactly as

$$\beta_{L,R} = \frac{N_c}{8\pi^2} |F^{t_L, t_R}|^4 \left[\frac{m_{Q_1}^2 + m_{Q_5}^2}{2(m_{Q_1}^2 - m_{Q_5}^2)} \log \left(\frac{m_{Q_1}^2}{m_{Q_5}^2} \right) - 1 \right], \quad (\text{C.20})$$

and

$$\epsilon = \frac{N_c}{8\pi^2} |F^{t_L}|^2 |F^{t_R}|^2 \left[1 - \cos \theta_{\text{phase}} \frac{m_{Q_1} m_{Q_5}}{m_{Q_1}^2 - m_{Q_5}^2} \log \left(\frac{m_{Q_1}^2}{m_{Q_5}^2} \right) \right]. \quad (\text{C.21})$$

References

- [1] G. F. Giudice, G. Isidori, A. Salvio and A. Strumia, *Softened Gravity and the Extension of the Standard Model up to Infinite Energy*, *JHEP* **02** (2015) 137, [[1412.2769](#)].
- [2] ATLAS collaboration, G. Aad et al., *Observation of a new particle in the search for the Standard Model Higgs boson with the ATLAS detector at the LHC*, *Phys. Lett.* **B716** (2012) 1–29, [[1207.7214](#)].
- [3] CMS collaboration, S. Chatrchyan et al., *Observation of a new boson at a mass of 125 GeV with the CMS experiment at the LHC*, *Phys. Lett.* **B716** (2012) 30–61, [[1207.7235](#)].
- [4] D. B. Kaplan and H. Georgi, *SU(2) \times U(1) Breaking by Vacuum Misalignment*, *Phys. Lett.* **B136** (1984) 183–186.
- [5] M. J. Dugan, H. Georgi and D. B. Kaplan, *Anatomy of a Composite Higgs Model*, *Nucl. Phys.* **B254** (1985) 299–326.
- [6] R. Contino, *The Higgs as a Composite Nambu-Goldstone Boson*, in *Physics of the large and the small, TASI 09, proceedings of the Theoretical Advanced Study Institute in Elementary Particle Physics, Boulder, Colorado, USA, 1-26 June 2009*, pp. 235–306, 2011. [1005.4269](#). DOI.
- [7] G. Panico and A. Wulzer, *The Composite Nambu-Goldstone Higgs*, *Lect. Notes Phys.* **913** (2016) pp.1–316, [[1506.01961](#)].
- [8] C. Csaki and P. Tanedo, *Beyond the Standard Model*, in *Proceedings, 2013 European School of High-Energy Physics (ESHEP 2013): Paradfurdo, Hungary, June 5-18, 2013*, pp. 169–268, 2015. [1602.04228](#). DOI.
- [9] G. F. Giudice, C. Grojean, A. Pomarol and R. Rattazzi, *The Strongly-Interacting Light Higgs*, *JHEP* **06** (2007) 045, [[hep-ph/0703164](#)].
- [10] A. Pomarol and F. Riva, *The Composite Higgs and Light Resonance Connection*, *JHEP* **08** (2012) 135, [[1205.6434](#)].
- [11] G. Panico, M. Redi, A. Tesi and A. Wulzer, *On the Tuning and the Mass of the Composite Higgs*, *JHEP* **03** (2013) 051, [[1210.7114](#)].
- [12] P. R. Archer, *Fine Tuning in the Holographic Minimal Composite Higgs Model*, [1403.8048](#).
- [13] J. Barnard and M. White, *Collider constraints on tuning in composite Higgs models*, *JHEP* **10** (2015) 072, [[1507.02332](#)].
- [14] C. Csaki, T. Ma and J. Shu, *The Maximally Symmetric Composite Higgs*, [1702.00405](#).

- [15] J. Barnard, D. Murnane, M. White and A. G. Williams, *Constraining fine tuning in Composite Higgs Models with partially composite leptons*, [1703.07653](#).
- [16] ATLAS COLLABORATION collaboration, *Search for new physics using events with b-jets and a pair of same charge leptons in 3.2 fb^{-1} of pp collisions at $\sqrt{s} = 13\text{ TeV}$ with the ATLAS detector*, Tech. Rep. ATLAS-CONF-2016-032, CERN, Geneva, Jun, 2016.
- [17] T. Gherghetta, B. von Harling, A. D. Medina and M. A. Schmidt, *The Scale-Invariant NMSSM and the 126 GeV Higgs Boson*, *JHEP* **02** (2013) 032, [[1212.5243](#)].
- [18] F. Brummer, S. Kraml and S. Kulkarni, *Anatomy of maximal stop mixing in the MSSM*, *JHEP* **08** (2012) 089, [[1204.5977](#)].
- [19] R. Contino, L. Da Rold and A. Pomarol, *Light custodians in natural composite Higgs models*, *Phys. Rev.* **D75** (2007) 055014, [[hep-ph/0612048](#)].
- [20] A. Azatov and J. Galloway, *Light Custodians and Higgs Physics in Composite Models*, *Phys. Rev.* **D85** (2012) 055013, [[1110.5646](#)].
- [21] O. Matsedonskyi, G. Panico and A. Wulzer, *Light Top Partners for a Light Composite Higgs*, *JHEP* **01** (2013) 164, [[1204.6333](#)].
- [22] K. Agashe, R. Contino and A. Pomarol, *The Minimal composite Higgs model*, *Nucl. Phys.* **B719** (2005) 165–187, [[hep-ph/0412089](#)].
- [23] K. Agashe and R. Contino, *The Minimal composite Higgs model and electroweak precision tests*, *Nucl. Phys.* **B742** (2006) 59–85, [[hep-ph/0510164](#)].
- [24] J. Barnard, T. Gherghetta, A. Medina and T. S. Ray, *Radiative corrections to the composite Higgs mass from a gluon partner*, *JHEP* **10** (2013) 055, [[1307.4778](#)].
- [25] A. Carmona and F. Goertz, *A naturally light Higgs without light Top Partners*, *JHEP* **05** (2015) 002, [[1410.8555](#)].
- [26] A. Carmona and F. Goertz, *Composite Taus and Higgs Decays*, *PoS EPS-HEP2013* (2013) 267, [[1310.3825](#)].
- [27] B. Gripaios, A. Pomarol, F. Riva and J. Serra, *Beyond the Minimal Composite Higgs Model*, *JHEP* **04** (2009) 070, [[0902.1483](#)].
- [28] J. Galloway, J. A. Evans, M. A. Luty and R. A. Tacchi, *Minimal Conformal Technicolor and Precision Electroweak Tests*, *JHEP* **10** (2010) 086, [[1001.1361](#)].
- [29] J. Mrazek, A. Pomarol, R. Rattazzi, M. Redi, J. Serra and A. Wulzer, *The Other Natural Two Higgs Doublet Model*, *Nucl. Phys.* **B853** (2011) 1–48, [[1105.5403](#)].
- [30] M. Chala, *$h \rightarrow \gamma\gamma$ excess and Dark Matter from Composite Higgs Models*, *JHEP* **01** (2013) 122, [[1210.6208](#)].
- [31] E. Bertuzzo, T. S. Ray, H. de Sandes and C. A. Savoy, *On Composite Two Higgs Doublet Models*, *JHEP* **05** (2013) 153, [[1206.2623](#)].

- [32] M. Chala, G. Nardini and I. Sobolev, *Unified explanation for dark matter and electroweak baryogenesis with direct detection and gravitational wave signatures*, *Phys. Rev.* **D94** (2016) 055006, [[1605.08663](#)].
- [33] M. Redi and A. Tesi, *Implications of a Light Higgs in Composite Models*, *JHEP* **10** (2012) 166, [[1205.0232](#)].
- [34] J. Serra, *Beyond the Minimal Top Partner Decay*, *JHEP* **09** (2015) 176, [[1506.05110](#)].
- [35] M. Low, A. Tesi and L.-T. Wang, *A pseudoscalar decaying to photon pairs in the early LHC Run 2 data*, *JHEP* **03** (2016) 108, [[1512.05328](#)].
- [36] H. Cai, T. Flacke and M. Lespinasse, *A composite scalar hint from di-boson resonances?*, [1512.04508](#).
- [37] A. Arbey, G. Cacciapaglia, H. Cai, A. Deandrea, S. Le Corre and F. Sannino, *Fundamental Composite Electroweak Dynamics: Status at the LHC*, *Phys. Rev.* **D95** (2017) 015028, [[1502.04718](#)].
- [38] M. Frigerio, A. Pomarol, F. Riva and A. Urbano, *Composite Scalar Dark Matter*, *JHEP* **07** (2012) 015, [[1204.2808](#)].
- [39] D. Marzocca and A. Urbano, *Composite Dark Matter and LHC Interplay*, *JHEP* **07** (2014) 107, [[1404.7419](#)].
- [40] N. Fonseca, R. Zukanovich Funchal, A. Lessa and L. Lopez-Honorez, *Dark Matter Constraints on Composite Higgs Models*, *JHEP* **06** (2015) 154, [[1501.05957](#)].
- [41] M. Kim, S. J. Lee and A. Parolini, *WIMP Dark Matter in Composite Higgs Models and the Dilaton Portal*, [1602.05590](#).
- [42] J. R. Espinosa, B. Gripaios, T. Konstandin and F. Riva, *Electroweak Baryogenesis in Non-minimal Composite Higgs Models*, *JCAP* **1201** (2012) 012, [[1110.2876](#)].
- [43] E. Katz, A. E. Nelson and D. G. E. Walker, *The Intermediate Higgs*, *JHEP* **08** (2005) 074, [[hep-ph/0504252](#)].
- [44] J. Barnard, T. Gherghetta and T. S. Ray, *UV descriptions of composite Higgs models without elementary scalars*, *JHEP* **02** (2014) 002, [[1311.6562](#)].
- [45] G. Ferretti and D. Karateev, *Fermionic UV completions of Composite Higgs models*, *JHEP* **03** (2014) 077, [[1312.5330](#)].
- [46] G. Cacciapaglia and F. Sannino, *Fundamental Composite (Goldstone) Higgs Dynamics*, *JHEP* **04** (2014) 111, [[1402.0233](#)].
- [47] A. Agugliaro, O. Antipin, D. Becciolini, S. De Curtis and M. Redi, *UV complete composite Higgs models*, *Phys. Rev.* **D95** (2017) 035019, [[1609.07122](#)].
- [48] J. Galloway, A. L. Kagan and A. Martin, *A UV complete partially composite-pNGB Higgs*, *Phys. Rev.* **D95** (2017) 035038, [[1609.05883](#)].

- [49] C. Niehoff, P. Stangl and D. M. Straub, *Electroweak symmetry breaking and collider signatures in the next-to-minimal composite Higgs model*, *JHEP* **04** (2017) 117, [[1611.09356](#)].
- [50] C. G. Callan, Jr., S. R. Coleman, J. Wess and B. Zumino, *Structure of phenomenological Lagrangians. 2.*, *Phys. Rev.* **177** (1969) 2247–2250.
- [51] S. R. Coleman, J. Wess and B. Zumino, *Structure of phenomenological Lagrangians. 1.*, *Phys. Rev.* **177** (1969) 2239–2247.
- [52] D. Marzocca, M. Serone and J. Shu, *General Composite Higgs Models*, *JHEP* **08** (2012) 013, [[1205.0770](#)].
- [53] D. Pappadopulo, A. Thamm and R. Torre, *A minimally tuned composite Higgs model from an extra dimension*, *JHEP* **07** (2013) 058, [[1303.3062](#)].
- [54] D. Buarque Franzosi, G. Cacciapaglia, H. Cai, A. Deandrea and M. Frandsen, *Vector and Axial-vector resonances in composite models of the Higgs boson*, *JHEP* **11** (2016) 076, [[1605.01363](#)].
- [55] M. Chaichian, A. Datta, K. Huitu and Z.-h. Yu, *Radion and Higgs mixing at the LHC*, *Phys. Lett.* **B524** (2002) 161–169, [[hep-ph/0110035](#)].
- [56] D. Dominici, B. Grzadkowski, J. F. Gunion and M. Toharia, *The Scalar sector of the Randall-Sundrum model*, *Nucl. Phys.* **B671** (2003) 243–292, [[hep-ph/0206192](#)].
- [57] N. Desai, U. Maitra and B. Mukhopadhyaya, *An updated analysis of radion-higgs mixing in the light of LHC data*, *JHEP* **10** (2013) 093, [[1307.3765](#)].
- [58] K. S. Babu, C. F. Kolda and J. March-Russell, *Implications of generalized Z - Z-prime mixing*, *Phys. Rev.* **D57** (1998) 6788–6792, [[hep-ph/9710441](#)].
- [59] K. Agashe, R. Contino, L. Da Rold and A. Pomarol, *A Custodial symmetry for $Zb\bar{b}$* , *Phys. Lett.* **B641** (2006) 62–66, [[hep-ph/0605341](#)].
- [60] H. Georgi, D. B. Kaplan and L. Randall, *Manifesting the Invisible Axion at Low-energies*, *Phys. Lett.* **B169** (1986) 73–78.
- [61] K. S. Jeong, Y. Shoji and M. Yamaguchi, *Singlet-Doublet Higgs Mixing and Its Implications on the Higgs mass in the PQ-NMSSM*, *JHEP* **09** (2012) 007, [[1205.2486](#)].
- [62] K. Agashe, R. Contino and R. Sundrum, *Top compositeness and precision unification*, *Phys. Rev. Lett.* **95** (2005) 171804, [[hep-ph/0502222](#)].
- [63] A. Falkowski, F. Riva and A. Urbano, *Higgs at last*, *JHEP* **11** (2013) 111, [[1303.1812](#)].
- [64] R. Barbieri, B. Bellazzini, V. S. Rychkov and A. Varagnolo, *The Higgs boson from an extended symmetry*, *Phys. Rev.* **D76** (2007) 115008, [[0706.0432](#)].
- [65] ATLAS, CMS collaboration, G. Aad et al., *Measurements of the Higgs boson production and decay rates and constraints on its couplings from a combined ATLAS and CMS analysis of the LHC pp collision data at $\sqrt{s} = 7$ and 8 TeV*, *JHEP* **08** (2016) 045, [[1606.02266](#)].

- [66] CMS collaboration, *Projected Performance of an Upgraded CMS Detector at the LHC and HL-LHC: Contribution to the Snowmass Process*, in *Proceedings, Community Summer Study 2013: Snowmass on the Mississippi (CSS2013): Minneapolis, MN, USA, July 29-August 6, 2013*, 2013. [1307.7135](#).
- [67] *Projections for measurements of Higgs boson signal strengths and coupling parameters with the ATLAS detector at a HL-LHC*, Tech. Rep. ATL-PHYS-PUB-2014-016, CERN, Geneva, Oct, 2014.
- [68] G. J. Gounaris and F. M. Renard, *Remarkable signals of t_R compositeness*, [1611.02426](#).
- [69] F. M. Renard, *$t_{L,R}$ inclusive distributions as tests of top compositeness*, [1701.03382](#).
- [70] B. Bellazzini, C. Csaki, J. Hubisz, J. Serra and J. Terning, *Composite Higgs Sketch*, *JHEP* **11** (2012) 003, [[1205.4032](#)].